



## A Study of Preliminary Design Methods for Low Noise Fans

L. Danielle Koch<sup>1</sup>  
NASA Glenn Research Center  
21000 Brookpark Road  
Cleveland, OH 44135

### ABSTRACT

*Engineers need theory and computer codes to help them design quiet and efficient fans. A fast method to identify low-noise stator vane counts that might minimize tone noise for axial ducted fans has been developed. The analysis begins with a preliminary aerodynamic fan design. Duct acoustic and rotor-stator interaction theories are combined to predict the set of cut-on circumferential modes that are expected to be generated and propagate through the fan duct. By predicting the number of cut-on circumferential modes for each vane count, a set of low-noise vane counts for a given rotor and duct design can be identified. This method was used to design the stator set for NASA's spacecraft cabin ventilation fan, in order to minimize tone noise generated by rotor-stator interaction at the first three blade passing frequency harmonics. This method was also applied to three other research fans that NASA uses for aeroacoustics research for comparison. This technique can be used to include acoustic design criteria early in the design of an axial fan and provide valuable information to guide the final design of quiet fans.*

### 1. INTRODUCTION

Quiet spacecraft cabin ventilation fans are needed for ambitious long duration space exploration missions. A spacecraft cabin ventilation fan prototype, shown in Figure 1, is currently being used in an aeroacoustic research project at NASA Glenn Research Center (GRC) and NASA Johnson Space Center (JSC).<sup>1</sup> In this report, a fast method for identifying stator vane counts that could help minimize tone noise generated for this fan is described. The preliminary aerodynamic design of a fan was used as a starting point for this acoustic design technique and the spacecraft cabin ventilation fan is used as an example. Drawing on design paradigms for turbofan engines,

---

<sup>1</sup> L.Danielle.Koch@nasa.gov

#### Notice for Copyrighted Information

This manuscript is a work of the United States Government authored as part of the official duties of employee(s) of the National Aeronautics and Space Administration. No copyright is claimed in the United States under Title 17, U.S. Code. All other rights are reserved by the United States Government. Any publisher accepting this manuscript for publication acknowledges that the United States Government retains a non-exclusive, irrevocable, worldwide license to prepare derivative works, publish, or reproduce the published form of this manuscript, or allow others to do so, for United States government purposes.

this technique then combines results from classic duct theory from Morse and Ingard<sup>2</sup> and rotor-stator interaction theory from Tyler and Sofrin.<sup>3</sup> Results of the spacecraft cabin ventilation fan acoustic analysis is presented, along with the final aerodynamic and acoustic design of the fan. This acoustic design method was also used to analyze three other fans NASA uses for aeroacoustic research: the Advanced Noise Control Fan (ANCF),<sup>4</sup> the Advanced Ducted Propulsor (ADP),<sup>5</sup> and the Source Diagnostic Test (SDT) Fan.<sup>6</sup> Results from all four fans are compared and discussed.

This fast method can be used to include acoustic design criteria early in the design of an axial fan and provide valuable information to guide the final design of quieter fans. Circumferential mode sound power levels are not estimated in this technique for identifying potentially advantageous blade-vane counts for a fan. Future research is suggested, highlighting the attempts made to use theory to from Sofrin and Mathews.<sup>7</sup>

## 2. PRELIMINARY AERODYNAMIC DESIGN OF THE SPACECRAFT CABIN VENTILATION FAN

A preliminary aerodynamic design of the spacecraft cabin ventilation fan was generated by Daniel Tweedt, given design goals from NASA.<sup>8,9</sup> The design goals for the spacecraft cabin vent fan are given below in Table 1, along with the preliminary design values for a few important dimensions and operating conditions.

## 3. ACOUSTIC DESIGN METHOD

The first part of this acoustic design method is to determine which circumferential modes are cut-on and which circumferential modes are cut-off for a given rotor and duct. The solution to the convective wave equation is used to characterize the propagation of sound through circular and annular ducts with hard walls and a mean flow. The reader is referred to Morse and Ingard<sup>2</sup> for a thorough derivation of this solution. Relevant input to this analysis includes the rotor hub radius ( $R_{hub}$ ), duct radius ( $R_{duct}$ ), circumferential ( $m$ ) and radial ( $\mu$ ) mode order number. Output from this calculation includes the eigenvalues for each duct mode ( $\alpha_{m,\mu}$ ). The cut-off frequency ( $(f_{co})_{m,\mu}$ ) and the cut-off ratio ( $\zeta_{m,\mu}$ ) can be then calculated using the eigenvalues for each mode ( $\alpha_{m,\mu}$ ), the BPF harmonic index ( $n$ ), the number of rotor blades ( $B$ ), rotor blade passing frequency ( $f$ ), and the axial Mach number ( $M$ ) of the flow through the fan. With this information, the set of cut-on and cut-off circumferential modes can be determined for a given ducted rotor. This calculation is not dependent upon the number of stator vanes. In these calculations, we examined trends for the first radial mode only,  $\mu=1$ . Circumferential modes propagate when the cut-off ratio is greater than 1.

$$(f_{co})_{m,\mu} = \frac{c_0 \alpha_{m,\mu}}{2R_{duct}} \sqrt{1 - M^2} \quad (1)$$

$$\zeta_{m,\mu} = f / f_{co,m,\mu} \quad (2)$$

The second part of this acoustic design method is to determine which circumferential modes are generated by the interaction of rotor wakes with stator vanes. Tyler and Sofrin<sup>3</sup> derived a relationship (Eq.3) for the rotor-stator interaction modes of ducted fans, where  $m$  is the circumferential mode number,  $n$  is the harmonic number,  $B$  is the number of rotor blades,  $k$  is an index, and  $V$  is the number of stator vanes. All variables in this equation are integers.

Now that we know which circumferential modes can propagate through the duct and which circumferential modes are generated, we can count the number of cut-on modes for a given rotor with different stator vane counts. We will use the spacecraft cabin vent fan to illustrate this. Figure 2 shows a plot of circumferential mode number versus the number of stator

vanes for the 1 BPF tone for the spacecraft vent fan (see parameters in Table 1). Using the Tyler Sofrin equation (Eq. 3), varying  $k$  and  $V$ , we see that the y-axis intercept value is equal to  $nB$ . The cut-off circumferential modes,  $m_{cutoff}$ , are found from the duct acoustics computation. For the spacecraft cabin vent fan circumferential modes greater than 2 and less than -2 are cut-off for 1 BPF. In Figure 2, the minimum y-axis value is set equal to -2 corresponding to one of the duct cut-off modes. The maximum value of  $k$  is chosen to be -1 and the minimum value of  $k$ ,  $k_{min}$ , is found by solving the Tyler and Sofrin equation setting  $V = 1$ . The modes generated by the fan are computed by varying the number of vanes,  $V$ , from 0 to  $V_{cutoff}$ , which is where the  $k=-1$  line intersects with  $y = m_{cutoff}$ , as we describe above. The number of cut-on circumferential modes can be counted for different values of  $V$ , as shown in Figure 4. Advantageous vane counts are those that do not have any (or few) cut-on circumferential modes, for a given number of rotor blades, rotor speed, and duct size.

$$m = nB + kV \quad (3)$$

$$m_{cutoff} = nB + (-1)V_{cutoff} = -2 \quad (4)$$

$$V_{cutoff} = \frac{(-2 - 1(9))}{-1} = 11 \quad (5)$$

$$m_{cutoff} = nB + k_{min}(1) = -2 \quad (6)$$

$$k_{min} = \frac{-2 - 1(9)}{1} = -11 \quad (7)$$

$$k_{min} = -V_{cutoff} \quad (8)$$

#### 4. FINAL DESIGN OF THE SPACECRAFT CABIN VENTILATION FAN

The final design of the spacecraft cabin vent fan featured 9 rotor blades and 11 stator vanes. Figures 5 and 6 are plots of frequency versus circumferential mode number, called “ $\mathcal{V}$ ” graphs here because of their shape, and are used to illustrate the relationship between the circumferential modes predicted to propagate through the duct (cut-on), the circumferential modes predicted to be evanescent and not propagate through the duct (cut-off), and the circumferential modes that are generated by the interaction between the rotor wakes with the stator vanes, for a given fan design. The “ $\mathcal{V}$ ” formed by lines with symbols represents the cut-off frequency for each duct circumferential mode and is determined by duct acoustics theory. When the frequency of the mode generated is greater than the cut-off frequency, the mode will be cut-on and will propagate through the duct, radiate to the farfield, and perceived as tone noise by an observer. The symbols without lines represent the circumferential modes generated by the rotor-stator interaction theory.<sup>3</sup> One way of interpreting this graph is that modes inside the “ $\mathcal{V}$ ” are cut-on and propagate through the duct. Modes outside the “ $\mathcal{V}$ ” are cut-off and do not propagate.

The “ $\mathcal{V}$ ” graph shown in Figure 5 illustrates that with a 9 bladed rotor and a stator with 11 vanes, that the tone at the first, second, and third BPF tone would be cut-off, and fourth BPF tone would be cut-on for circumferential mode number 3 at the design speed of 12,000 rpm. This was predicted to be an acoustic improvement over the preliminary aerodynamic design that featured a 9 bladed rotor paired with a stator with 13 vanes, shown in Figure 6. A stator with 13 vanes would generate a 3 BPF tone for circumferential mode number 1 and a 4 BPF tone at circumferential mode  $m=-3$ . Increasing the rotor speed to 13,600 rpm for both stator designs cut-on the circumferential mode  $m=-4$  for the third BPF harmonic, though this mode was not generated for either of these blade-vane counts at this rotor speed, so the variation in design speed had little effect to the final design in this range.

Examining the results plotted in Figures 7-12, the analysis indicates that a stator with 6, 7, or 11 or more vanes would cut off the first BPF tone for the spacecraft cabin vent fan. A stator

with 7, 11, 12, 13, 14, 15, or 21 or more vanes would cut off the second BPF tone. To cut off the third BPF tones, a stator would need to have 11, 21, 22, 23, or 31 or more vanes. Therefore, to cut off the first three BPF harmonics, stator designs with 11, 21, 22, 23, or 31 or more vanes should be considered. Ultimately, a stator with 11 vanes was chosen for the spacecraft cabin ventilation fan prototypes that have been fabricated for NASA.

## **5. COMPARISON WITH OTHER NASA FANS**

Results from the small spacecraft cabin ventilation fan are compared to three other larger fans that NASA uses to for aerodynamic and acoustic research, mainly for aircraft propulsion systems. The three fans are: the large low-speed Advanced Noise Control Fan (ANCF), the Advanced Ducted Propulsor (ADP), and the Source Diagnostic Test (SDT) fan. Images of the fans and their corresponding “*V*” graphs are shown in Figures 13 – 20. A summary of the four fans appears in Table 2 for quick comparison of key aerodynamic and acoustic features.

### **5.1 The Advanced Noise Control Fan**

The Advanced Noise Control Fan (ANCF), Figure 14, is a large low-speed ducted fan that has been used by NASA to perform a variety of aerodynamic and acoustic tests over the last 25 years. The ANCF rotor has 16 blades and rotates at 1800 rpm at the design point condition. The hub radius at the rotor blade leading edge is 18.75 cm (7.380 in) and the duct radius is 60.96 cm (24.00 in) at the rotor leading edge. Five stators have been built and tested: 13, 14, 15, 26, and 28 vanes. The circumferential modes that are predicted to be cut-on, cut-off, and generated by this fan are shown in the “*V*” graph of Figure 16 and listed in Table 2.

The results of the acoustic design method are shown in Figures 21-26. To cut off the first BPF tone, the ANCF stator could have 10, 11, 12, or 20 or more vanes. To cut off the second BPF tone, the ANCF stator could have 21, 22, 23, or 41 or more stator vanes. To cut off the third BPF tone, the ANCF stator would need 31, 32, 33, 34, or 62 or more vanes. Therefore, this analysis indicates that a stator with 21, 22, or 23 vanes would cut off the first and the second BPF tone for the ANCF. A stator with 31, 32, 33, 34, or 62 or more vanes would cut off the first and third BPF tone. To cut off the first three BPF tones, a stator would need 62 or more vanes.

### **5.2 The Advanced Ducted Propulsor**

The Advanced Ducted Propulsor (ADP) is a turbofan engine bypass fan model used by NASA to perform a variety of aerodynamic and acoustic tests in the NASA Glenn 9- by 15-ft Low Speed Wind Tunnel and is shown in Figure 17. The ADP includes a rotor with 18 blades that rotates at 5425 rpm at approach conditions. The hub radius at the rotor blade leading edge is 13.59 cm (5.349 in) and the duct radius is 27.94 cm (11.00 in) at the rotor leading edge. The fan exit guide vane has 45 vanes and there are 63 vanes in the core stator. The circumferential modes that are predicted to be cut-on by this fan are shown in the “*V*” graph of Figure 18 and listed in Table 2.

The results of the acoustic design method are shown in Figures 27-32. This analysis suggests that a stator with 25 vanes or more would cut off the first BPF tone for the ADP. A stator with 51 vanes would cut off the first and second BPF tone. To cut off the first three BPF tones, a stator would need to have 77 or more vanes.

### **5.3 The Source Diagnostic Test Fan**

The Source Diagnostic Test (SDT) Fan is also a turbofan engine bypass fan model used by NASA to perform a variety of aerodynamic and acoustic tests in the NASA Glenn 9- by 15-ft Low Speed Wind Tunnel and is shown in Figure 19. The SDT fan includes a rotor with 22

blades that rotates at 7808 rpm at approach conditions. The hub radius at the rotor blade leading edge is approximately 8.38 cm (3.30 in) and the duct radius is 27.91 cm (10.99 in). The fan exit guide vane has 54 vanes. The circumferential modes that are predicted to be cut-on by this fan are shown in the “*V*” graph of Figure 20 and listed in Table 2.

The results of the acoustic design method for the SDT fan are shown in Figures 33-38. The SDT fan was designed to cut off the first BPF tone only. The analysis in this report indicates that a stator with 36 vanes or more would cut off the first BPF tone for the SDT. A stator with 73 vanes would cut off the first and second BPF tone. To cut off the first three BPF tones, a stator would need to have 111 or more vanes.

## **6. RECOMMENDATIONS**

Analysis to estimate relative circumferential mode amplitudes developed by Sofrin and Mathews<sup>7</sup> was also explored during this research project, but a detailed description of the findings are beyond the scope of this report. Sofrin and Mathews<sup>7</sup> suggested that trends in rough estimates of the relative modal sound power for the circumferential modes of the first BPF would be useful. While this may be the case for the fan that they had been studying, a few comparisons with the measured sound power levels for the ANCF fan and the predictions for the ANCF from the V072 Rotor-Stator Interaction Tone Noise Prediction Code were not in agreement. Future efforts could revisit this theory.

## **7. CONCLUSION**

A fast method to identify low-noise stator vane counts that might minimize tone noise for axial ducted fans has been developed. This method was used to design the stator for NASA’s spacecraft cabin ventilation fan, which minimizes tone noise from rotor-stator interaction for the first three blade passing frequency harmonics. Using the preliminary aerodynamic design of a fan as a starting point, duct acoustic theory is combined with rotor-stator interaction theory to predict the set of cut-on circumferential modes that are expected to be generated and propagate through the fan duct. By counting the number of cut-on circumferential modes for each vane count, a set of low-noise vane counts for a given rotor and duct design can be identified. This method was also used to determine the set of low-noise vane counts for three other NASA research fans. This technique can be used to include acoustic design criteria early in the design of an axial fan and provide valuable information to guide the final design of low noise fans.

## **8. ACKNOWLEDGEMENTS**

This work was supported by NASA’s Advanced Exploration Systems International Space Station Habitation, Environmental Control and Life Support System project. The author thanks Dr. Daniel Sutliff (NASA GRC), Dr. Edmane Envia. (NASA GRC) and Jeffrey Severino (NASA GRC Pathways Intern) for their kind guidance and help with this research, especially with computing the duct mode cut-off frequencies.

## **9. REFERENCES**

1. Stephens, D., Goodman, Jonathan, Buehrle, R., Mirhashemi, A., Koch, L. D., Shook, T. D., Sutliff, D., Allen, C., S., M., Christopher, “Highlights of Aeroacoustic Tests of a Metal Spacecraft Cabin Vent Fan Prototype,” NASA-TM- 20220012622, 2022.
2. Morse, P. M., Ingard, K. U. *Theoretical acoustics* (Princeton University Press, 1986).
3. Tyler, J. M., Sofrin, T. G. “Axial Flow Compressor Noise Studies.” *SAE Transactions*, Vol. 70, pp. 309-332. 1962.
4. Sutliff, D. L. “Advanced noise control fan: A 20-year retrospective of contributions to aeroacoustics research.” *NASA/SP-2019-643*, 2019.

5. Heidelberg, L., Elliott, D., "A comparison of measured tone modes for two low noise propulsion fans," NASA TM- 2000-210231, AIAA-2000-1989, 2000.
6. Sutliff, D. L., "Source Diagnostic Fan II (22") Duct Mode Characteristics as Measured by the Rotating Rake Mode Measurement System while Operated in the NASA Glenn 9x15 Low Speed Wind Tunnel," AIAA 2022-3054, 2022.
7. Sofrin, T. G., Mathews, D. C. "Asymmetric Stator Interaction Noise." *Journal of Aircraft*, Vol. Vol. 17, Issue 8, pp. 554-560. 1979.
8. Tweedt, D. L. "Aerodynamic design and computational analysis of a space flight vehicle cabin ventilation fan." *The Journal of the Acoustical Society of America*, Vol. 127, No. 3, pp. 1838-1838. 2010.
9. Tweedt, D. L., "Aerodynamic Design and Computational Analysis of a Spaceflight Vehicle Cabin Ventilation Fan," NASA CR-2010-216329, 2010.

## 10. TABLES AND FIGURES

Table 1: Design Goals and Preliminary Aerodynamic Design of the Spacecraft Cabin Vent Fan

	Goals	Preliminary Aerodynamic Design Value
Flow rate	0.709 m <sup>3</sup> /s (150.3 cfm)	0.709 m <sup>3</sup> /s (150.3 cfm)
Total pressure rise	906 Pa (3.64 inches H <sub>2</sub> O)	925 Pa (3.716 inches of water)
Pressure	101 kPa (14.7 psia)	101 kPa (14.7 psia)
Temperature	21.1° C (70° F)	21.1° C (70° F)
Maximum diameter	0.102 m (4.0 in)	8.89 cm (3.50 in) flowpath diameter
Rotor hub diameter	Unconstrained	6.60 cm (2.60 in)
Maximum axial length	0.223 m (9.0 in)	0.223 m (9.0 in)
Rotor tip clearance gap	0.23 mm (0.009 in)	0.23 mm (0.009 in)
Rotor speed	Unconstrained	12,000 rpm to 13,600 rpm
Number of blades	Unconstrained	9
Number of vanes	Unconstrained	13
Rotor exit Mach number	Unconstrained	0.10 to 0.11 with approximately 35° swirl
Blade row spacing	Unconstrained	3.45 cm (1.37 in) approximately 2 rotor axial chord lengths

Table 2: Selected Design Features for Four NASA Research Fans

Fan	Spacecraft Cabin Ventilation Fan	Advanced Noise Control Fan (ANCF)	Advanced Ducted Propulsor (ADP)	Source Diagnostic Test (SDT) Fan
Operating Cond.	Design Point	Design Point	Approach	Approach
No. rotor blades	9	16	18	22
Rotor hub radius	1.30 in	7.380 in	5.349 in	3.30 in
Duct radius	1.75 in	24.00 in	11.00 in	10.99 in
Rotor speed	12,000 rpm	1,800 rpm	5,425 rpm	7,808 rpm
Axial Mach No.	M = 0.11	M = 0.10	MAS = 0.256	MAS=0.340
1 BPF Cut-on circum. modes	$-1 \leq m_{cuton} \leq 1$	$-4 \leq m_{cuton} \leq 4$	$-7 \leq m_{cuton} \leq 7$	$-13 \leq m_{cuton} \leq 13$
2 BPF Cut-on circum. modes	$-2 \leq m_{cuton} \leq 2$	$-9 \leq m_{cuton} \leq 9$	$-15 \leq m_{cuton} \leq 15$	$-28 \leq m_{cuton} \leq 28$
3 BPF Cut-on circum. modes	$-3 \leq m_{cuton} \leq 3$	$-14 \leq m_{cuton} \leq 14$	$-23 \leq m_{cuton} \leq 23$	$-44 \leq m_{cuton} \leq 44$
1 BPF Cut-off circum. modes	$m_{cutoff} \leq -2$ $m_{cutoff} \geq 2$	$m_{cutoff} \leq -5$ $m_{cutoff} \geq 5$	$m_{cutoff} \leq -8$ $m_{cutoff} \geq 8$	$m_{cutoff} \leq -14$ $m_{cutoff} \geq 14$
2 BPF Cut-off circum. modes	$m_{cutoff} \leq -3$ $m_{cutoff} \geq 3$	$m_{cutoff} \leq -10$ $m_{cutoff} \geq 10$	$m_{cutoff} \leq -16$ $m_{cutoff} \geq 16$	$m_{cutoff} \leq -29$ $m_{cutoff} \geq 29$
3 BPF Cut-off circum. modes	$m_{cutoff} \leq -4$ $m_{cutoff} \geq 4$	$m_{cutoff} \leq -15$ $m_{cutoff} \geq 15$	$m_{cutoff} \leq -24$ $m_{cutoff} \geq 24$	$m_{cutoff} \leq -45$ $m_{cutoff} \geq 45$

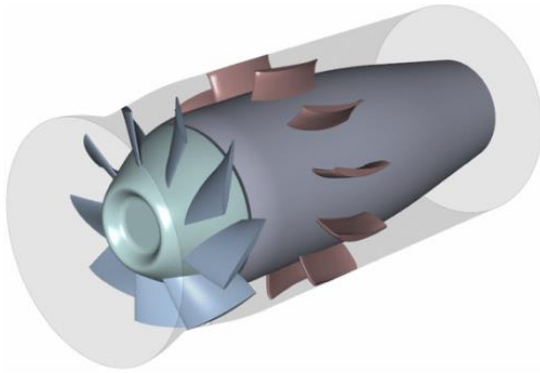


Figure 1: Final design of the spacecraft cabin ventilation fan with 9 rotor blades and 11 stator vanes. At design point conditions, the 1 BPF tone is cut-off for  $m = -1, 0$ , and 1.

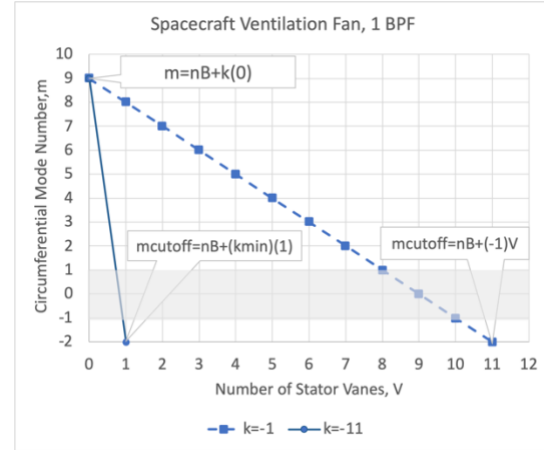


Figure 2: Example of a plot to find which circum. modes are cut-on for different number of stator vanes, The 1 BPF tone is cut-on for  $m = -1, 0, 1$ .

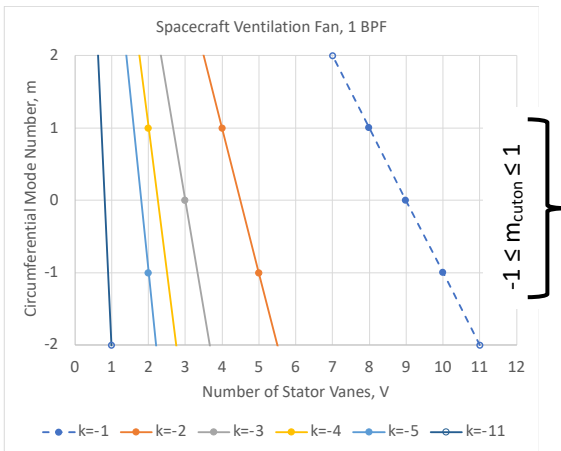


Figure 3: Close-up view of a plot to find which circum. modes are cut-on for different number of stator vanes, The 1 BPF tone is cut-on for  $m = -1, 0, 1$ .

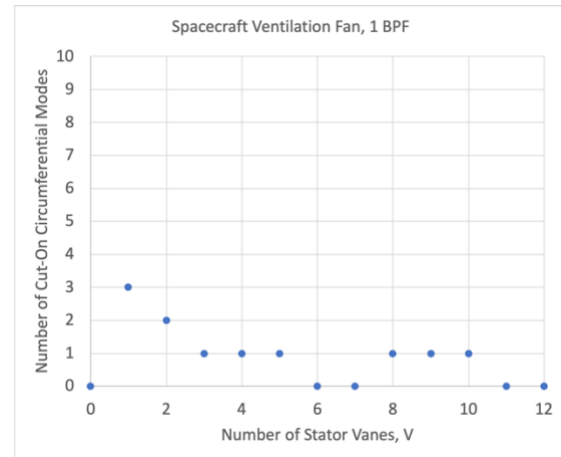


Figure 4: Example of a plot to find the number of cut-on circumferential modes for different numbers of stator vanes, 1 BPF, spacecraft cabin vent fan.

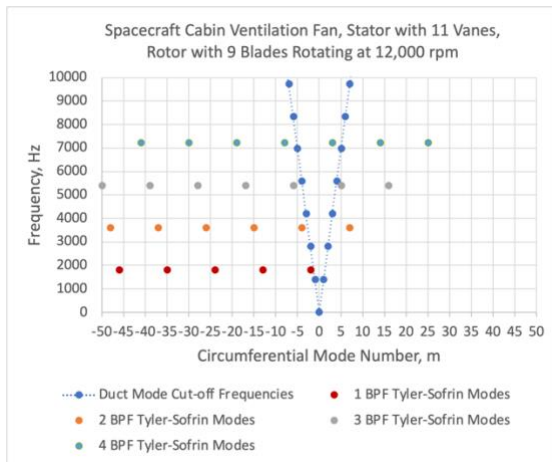


Figure 5: The "V" graph for final design of the spacecraft cabin ventilation fan.

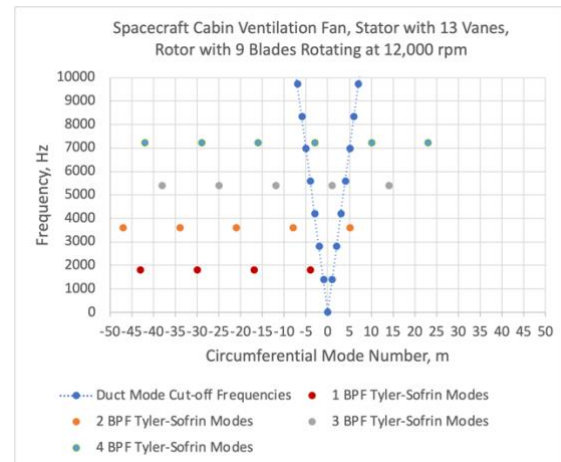


Figure 6: The "V" graph for the preliminary design of the spacecraft cabin ventilation fan.



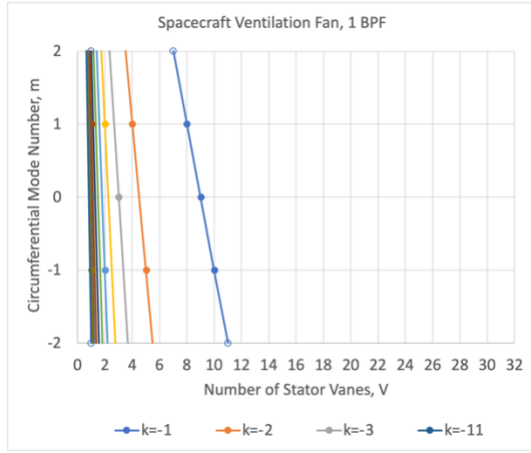


Figure 7: Circumferential modes cut-on for different numbers of stator vanes, 1 BPF, spacecraft vent fan. The 1 BPF tone is cut-on for  $m = -1, 0, 1$ .

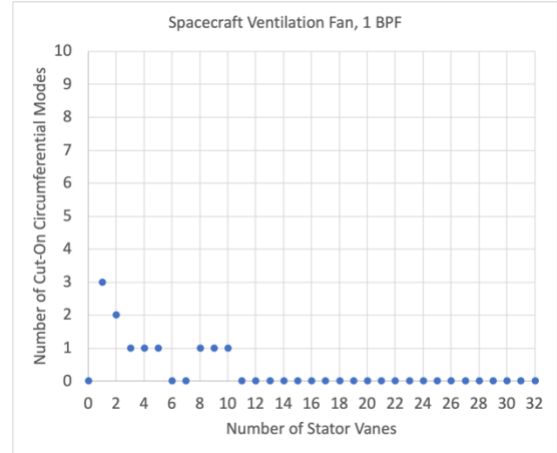


Figure 8: Number of cut-on circumferential modes for different numbers of stator vanes, 1 BPF, spacecraft cabin vent fan.

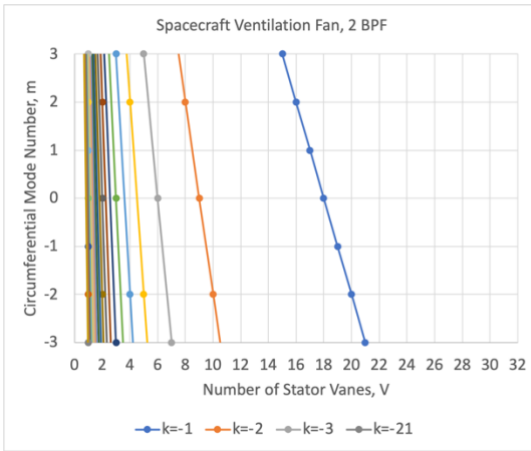


Figure 9: Circumferential modes cut-on for different numbers of stator vanes, 2 BPF, spacecraft vent fan. The 2 BPF tone is cut-on for  $m = -2$  to 2.

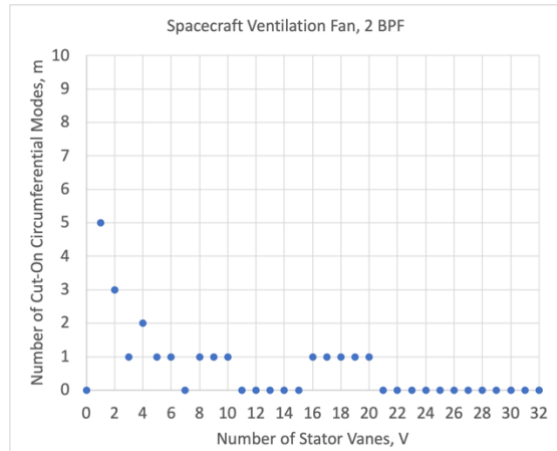


Figure 10: Number of cut-on circumferential modes for different numbers of stator vanes, 2 BPF, spacecraft cabin vent fan.

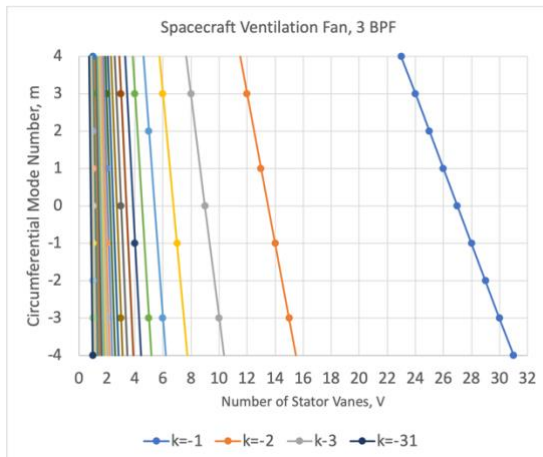


Figure 11: Circumferential modes cut-on for different numbers of stator vanes, 3 BPF, spacecraft vent fan. The 3 BPF tone is cut-on for  $m = -3$  to 3.

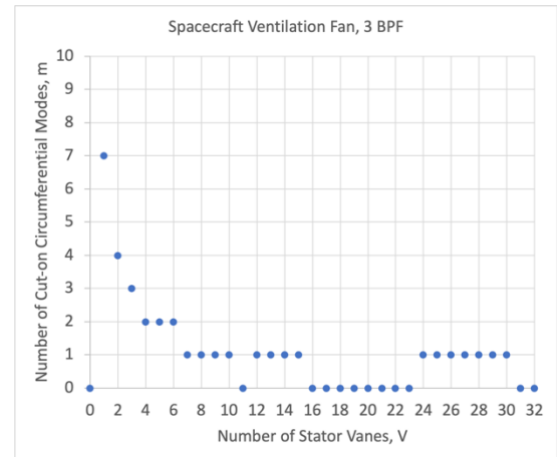


Figure 12: Number of cut-on circumferential modes for different numbers of stator vanes, 3 BPF, spacecraft cabin vent fan.



Figure 13: Spacecraft cabin ventilation fan

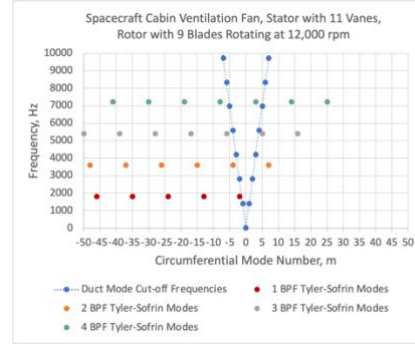


Figure 14: Spacecraft cabin vent fan "V" graph.

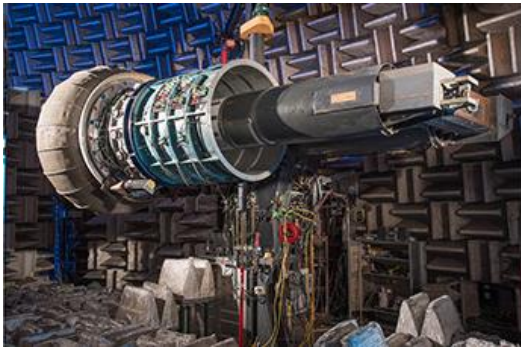


Figure 15: The Advanced Noise Control Fan (ANCF)

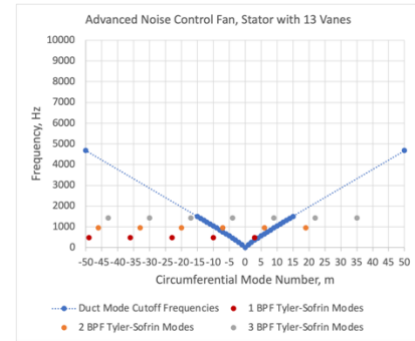


Figure 16: The ANCF "V" graph.



Figure 17: The Advanced Ducted Propulsor (ADP).

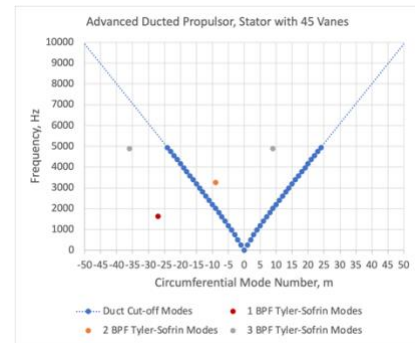


Figure 18: The ADP "V" graph.



Figure 19: The Source Diagnostics Test (SDT) fan.

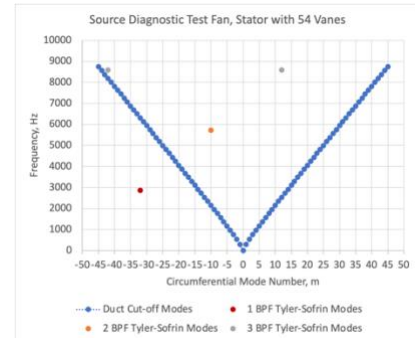


Figure 20: The SDT fan "V" graph.

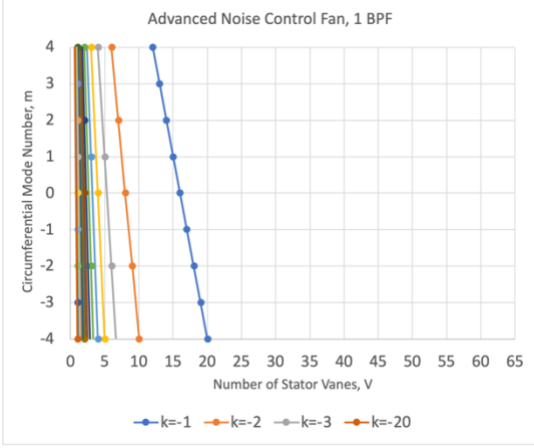


Figure 21: Circumferential modes cut-on for different numbers of stator vanes, 1 BPF, ANCF. The 1 BPF tone is cut-on for  $m = -3$  to 3.

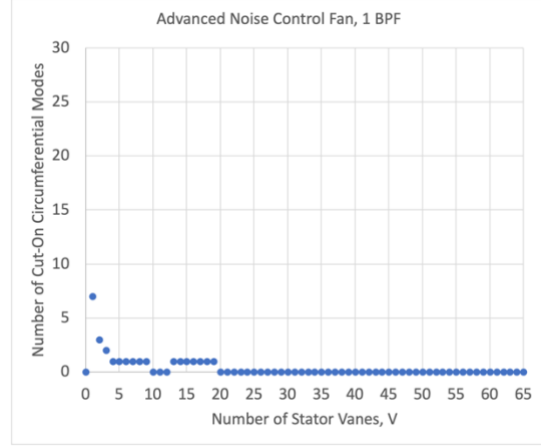


Figure 22: Number of cut-on circumferential modes for different numbers of stator vanes, 1 BPF, ANCF.

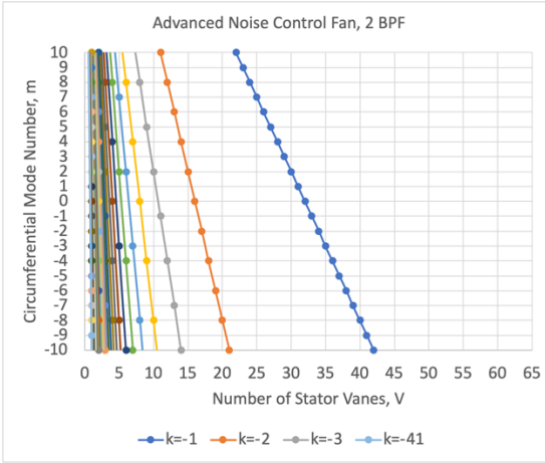


Figure 23: Circumferential modes cut-on for different numbers of stator vanes, 2 BPF, ANCF. The 2 BPF tone is cut-on for  $m = -9$  to 9.

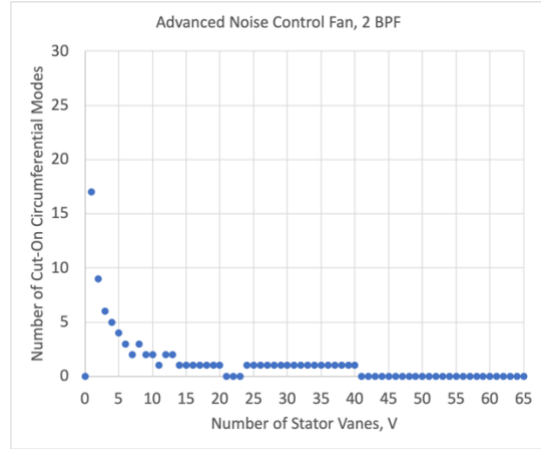


Figure 24: Number of cut-on circumferential modes for different numbers of stator vanes, 2 BPF, ANCF.

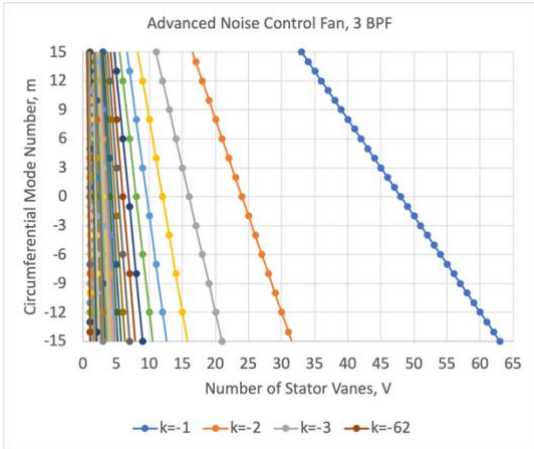


Figure 25: Circumferential modes cut-on for different numbers of stator vanes, 3 BPF, ANCF. The 3 BPF tone is cut-on for  $m = -14$  to 14.

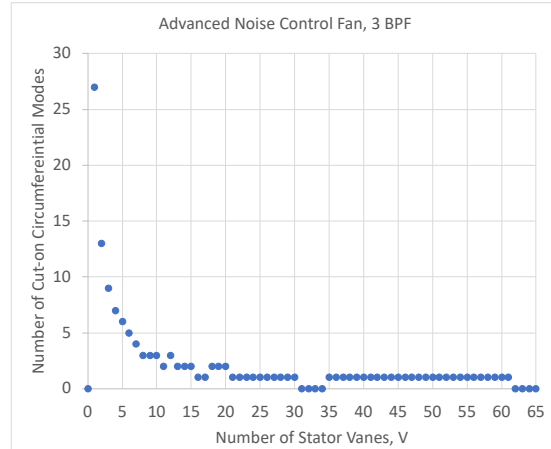


Figure 26: Number of cut-on circumferential modes for different numbers of stator vanes, 3 BPF, ANCF.

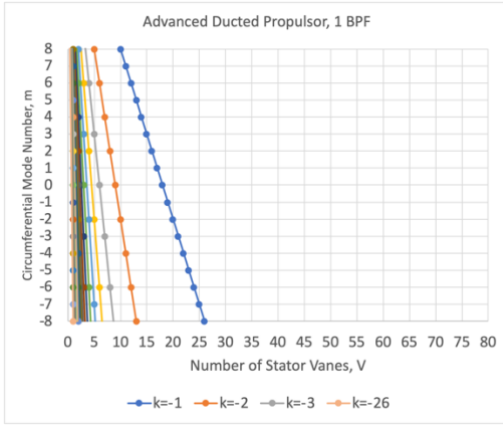


Figure 27: Circumferential modes cut-on for different numbers of stator vanes, 1 BPF, ADP. The 1 BPF tone is cut-on for  $m = -7$  to 7.

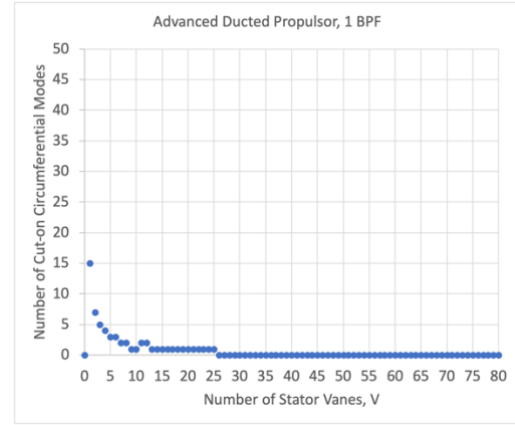


Figure 28: Number of cut-on circumferential modes for different numbers of stator vanes, 1 BPF, ADP.

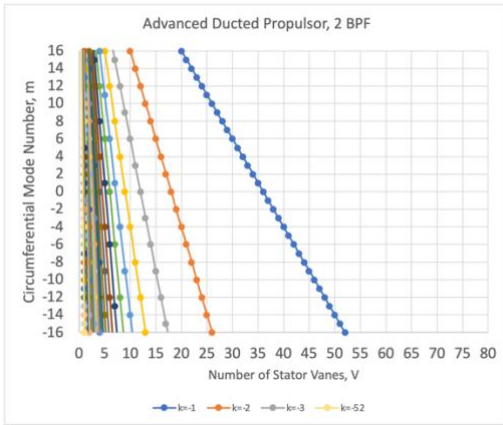


Figure 29: Circumferential modes cut-on for different numbers of stator vanes, 2 BPF, ADP. The 2 BPF tone is cut-on for  $m = -15$  to 15.

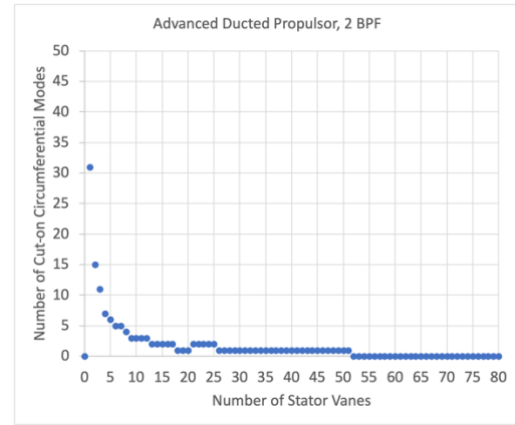


Figure 30: Number of cut-on circumferential modes for different numbers of stator vanes, 2 BPF, ADP.

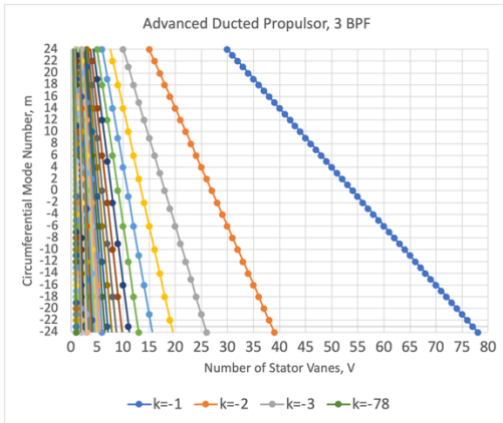


Figure 31: Circumferential modes for different numbers of stator vanes, 3 BPF, ADP. The 2 BPF tone is cut-on for  $m = -23$  to 23.

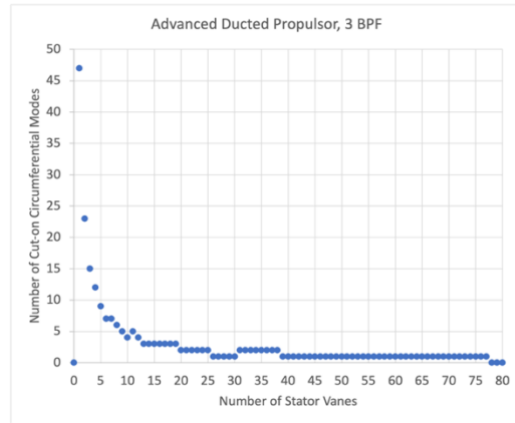


Figure 32: Number of cut-on circumferential modes for different numbers of stator vanes, 3 BPF, ADP.

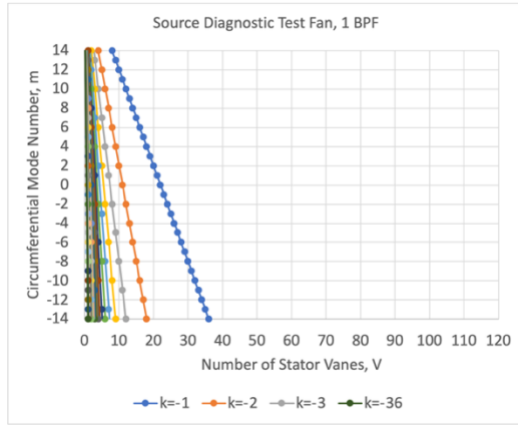


Figure 33: Circumferential modes cut-on for different numbers of stator vanes, 1 BPF, SDT fan. The 1 BPF tone is cut-on for  $m = -13$  to  $13$ .

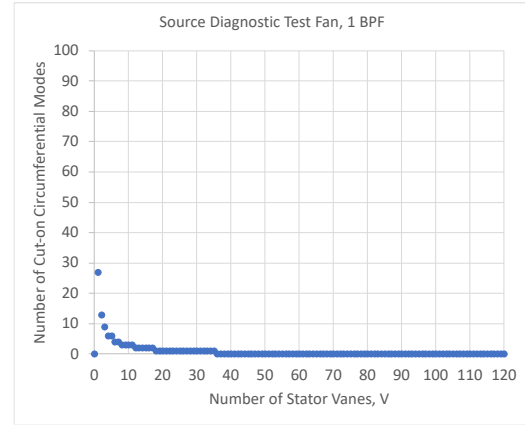


Figure 34: Number of cut-on circumferential modes for different numbers of stator vanes, 1 BPF, SDT fan.

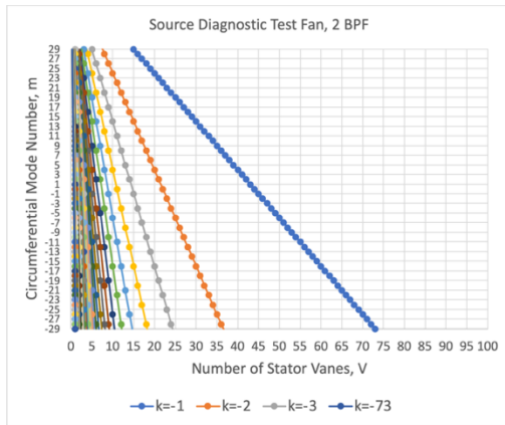


Figure 35: Circumferential modes cut-on for different numbers of stator vanes, 2 BPF, SDT fan. The 1 BPF tone is cut-on for  $m = -28$  to  $28$ .

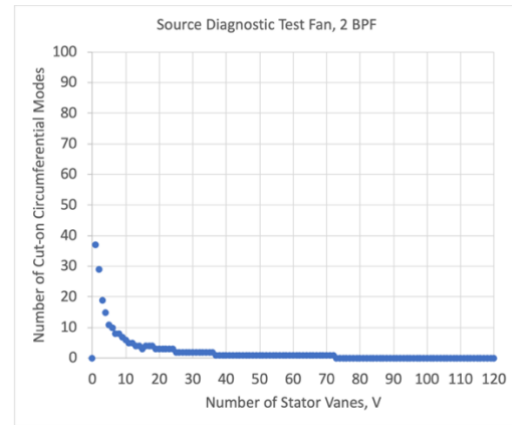


Figure 36: Number of cut-on circumferential modes for different numbers of stator vanes, 2 BPF, SDT fan.

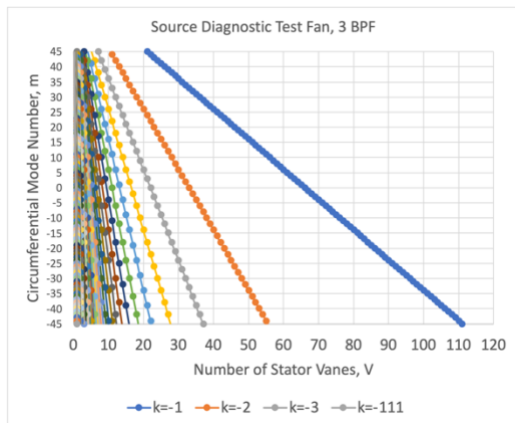


Figure 37: Circumferential modes cut-on for different numbers of stator vanes, 3 BPF, SDT fan. The 1 BPF tone is cut-on for  $m = -44$  to  $44$ .

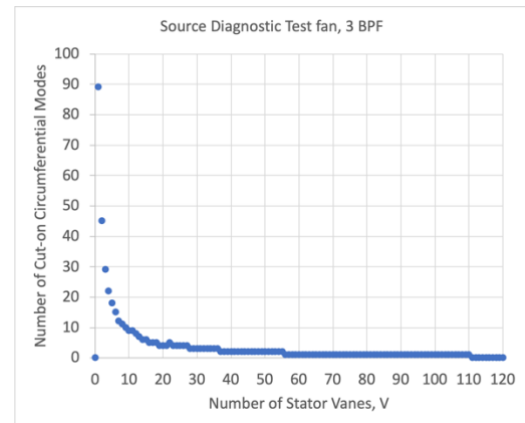


Figure 38: Number of cut-on circumferential modes for different numbers of stator vanes, 3 BPF, SDT fan.